

## Metrology for Future Energy Transmission

# WP4: METROLOGY FOR HVDC GRID CONDITION MONITORING

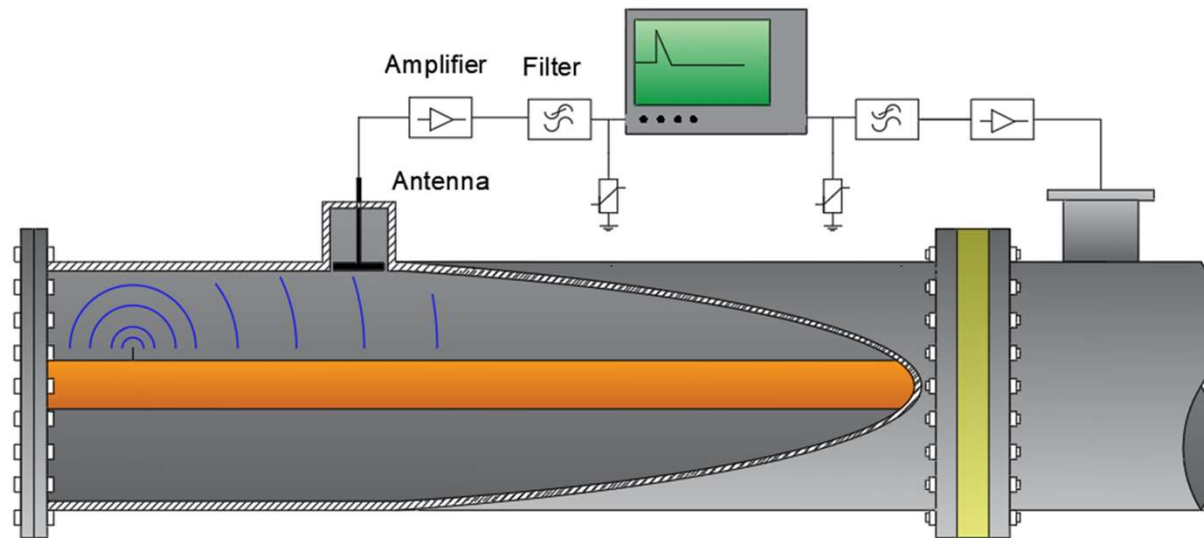
## TASK 4.2: PROCEDURE FOR CHARGE EVALUATION IN HVDC GIS USING MAGNETIC SENSORS MEASURING IN THE 30 - 300 MHZ RANGE

## Project Overview

Motivations:

- The increased need for gas-insulated substations (GIS) with remote monitoring.
- The IEC 60270 method is difficult to apply for onsite online substations.
- Unconventional methods do not provide a calibrated measurement.

This research focuses on an unconventional method in the very-high frequency range, aiming to measure calibrated online PD in on-site substations.



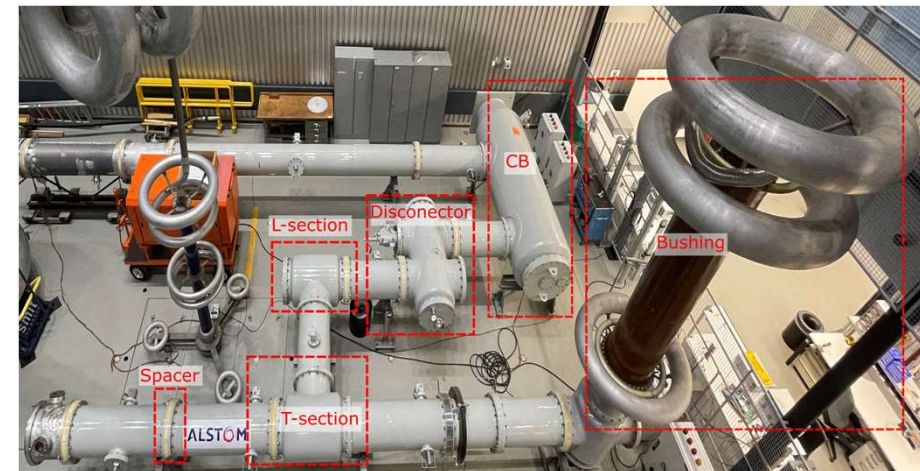
## Content

1. PD propagation in GIS
2. GIS artificial defects characterization.
3. Test Workbench
4. Sensor development
5. Characterization and Charge Estimation
6. Validation

# 1. PD pulse propagation in GIS

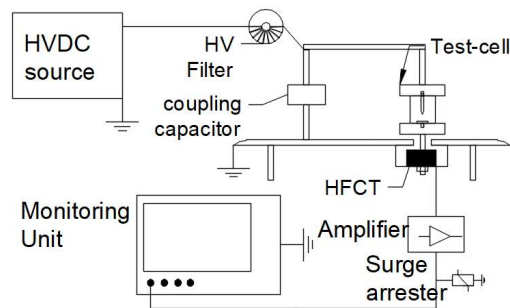
- For frequencies below the UHF the PD propagates in the transverse-electromagnetic mode, so the transmission line theory applies.

Discontinuity	$f < f_c$	$f > f_c$
<b>Straight line</b>	- Attenuation below 3dB/km. - Irregular current distribution near the source.	- TE attenuation below 4dB/km and TM below 10 dB/km - Sensor and PD source relative position attenuation. - Propagation modes speed difference attenuation.
<b>Spacer</b>	- Length and the characteristic impedance.	- Propagation modes speed difference attenuation.
<b>Change of diameter</b>	- Length and the characteristic impedance.	- Attenuated signal after the discontinuity.
<b>L section</b>	- Irregular current distribution near the change of direction.	- Attenuation at the by change of mode
<b>T section</b>	- Irregular current distribution near the change of direction. - 33% of attenuation after the T section	- Attenuation at the by change of mode
<b>Disconnecting Part</b>	- High attenuation, dependent on the gap length.	- Low attenuation, propagation in a circular waveguide.
<b>Bushing</b>	- high reflection due to the high characteristic impedance.	- high reflection due to the high characteristic impedance.



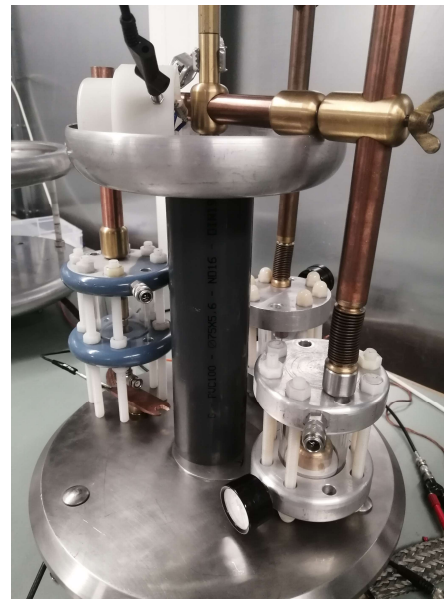
# 1. HVDC PD parameters

- The PD BW does not change after electric ageing for corona discharge, jumping particle, and Floating electrode. A change of BW was observed in SD. The PD BW determines the BW of the measuring system.
- Data set: PD amplitude, repetition rate, and pulse oscillography as a function of aging time.

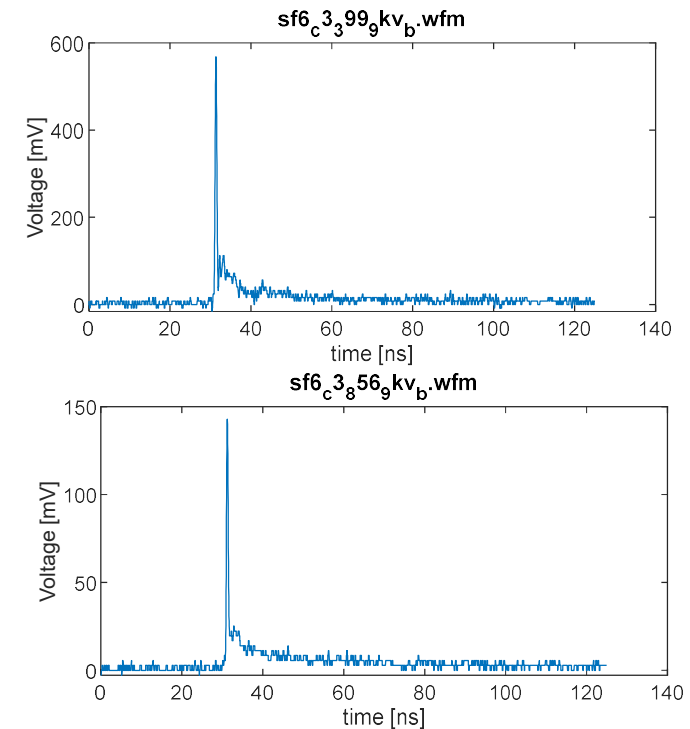


	Corona	FE	SD	JP
no ageing	>1000 MHz	>500 MHz	350 MHz	>500 MHz
end of ageing	>1000 MHz	>500 MHz	125 MHz	>500 MHz

Top: Test-setup for PD monitoring. Bottom: PD bandwidth before and after ageing.



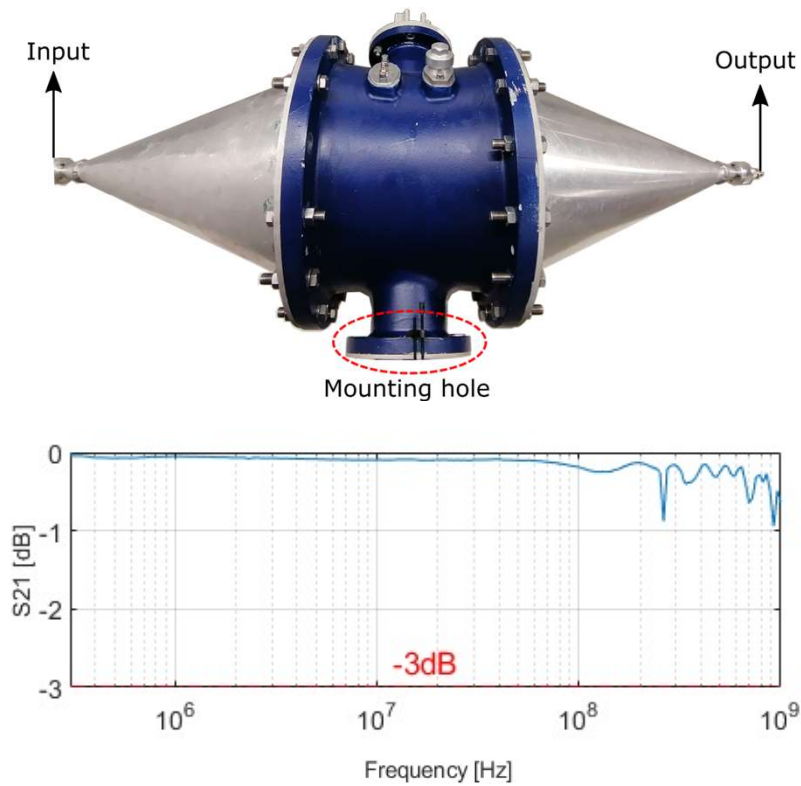
Test-setup picture for PD monitoring.



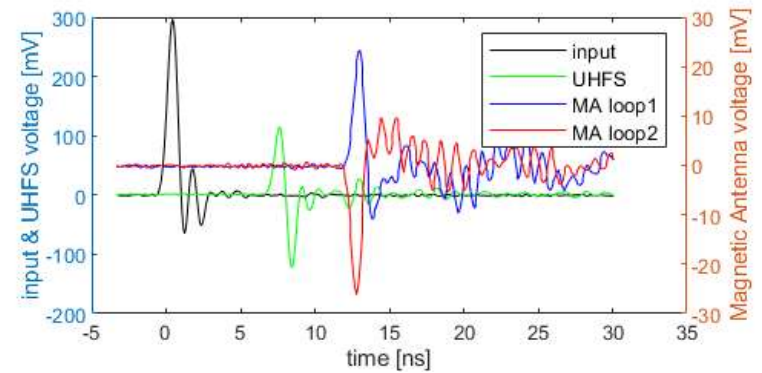
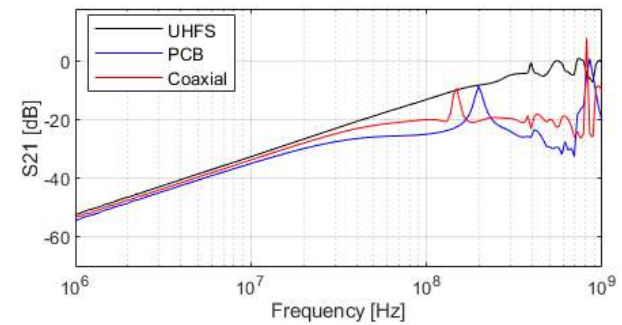
Top: aged corona defect after 339 hours. Bottom: aged corona defect after 856 hours.

## 2. Test Workbench

- 1GHz bandwidth workbench for PD sensors characterization.



Top: Test bench picture. Bottom: Testbench frequency response.



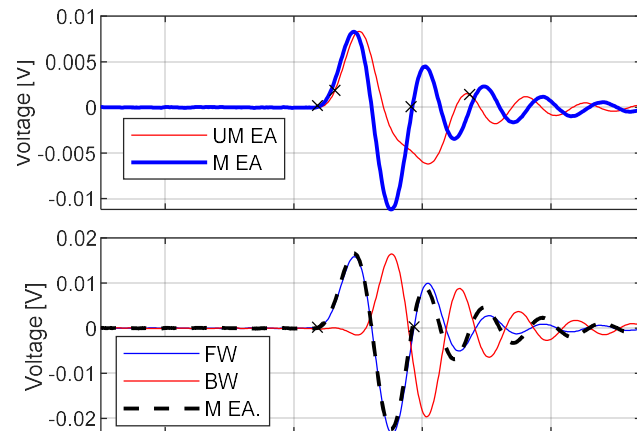
Top: Bode diagram of different antennas. Bottom: Time domain measurements for different antennas.



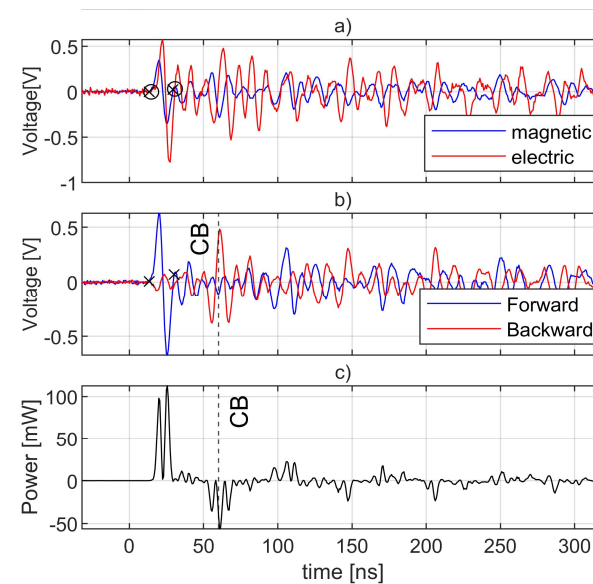


## 3.2. Sensor development

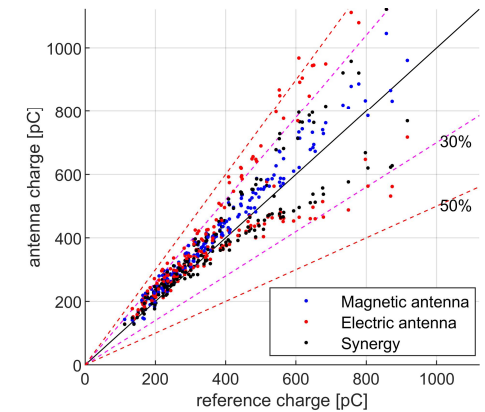
- Combination of VHF electric and magnetic sensor for PD power flow and reflection suppression for PD charge improvement.



Top: Overlapped pulse and matched pulse. Bottom: Forward and backward pulse and matched pulse.



PD measured with: a) magnetic and electric antenna, b) forward and backward pulses, c) power flow.



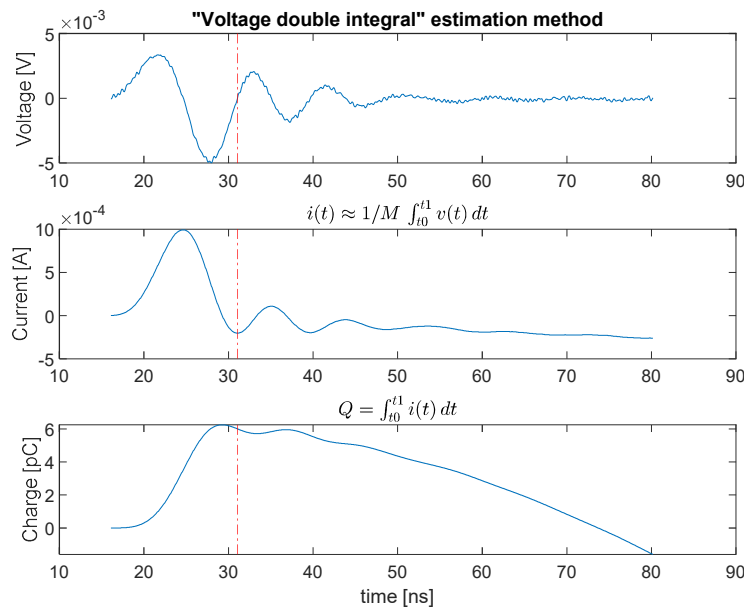
Antennas and synergy charges compared with reference charges for 200 PDs.



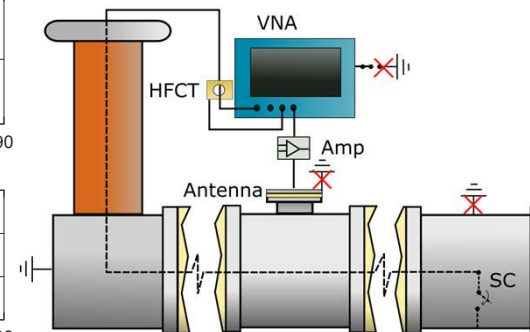
## 4. Charge Estimation procedure

- The voltage double integral method is based on the sensor's derivative response

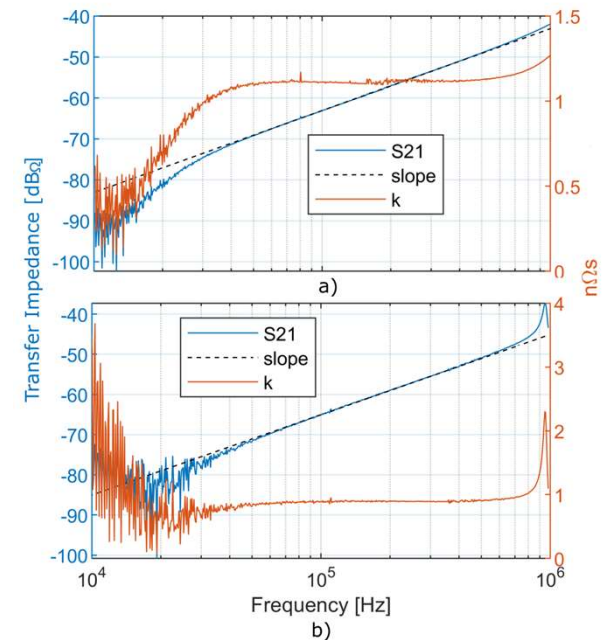
$$H(s) \approx \frac{sk}{s^2\omega_2^2 + s\omega_1 + 1} \quad Q \approx \frac{\iint u(t)dt^2}{k} \quad \left| \frac{dH(\omega)}{d\omega} \right|_{\omega \rightarrow 0} \approx k$$



Charge estimation development.



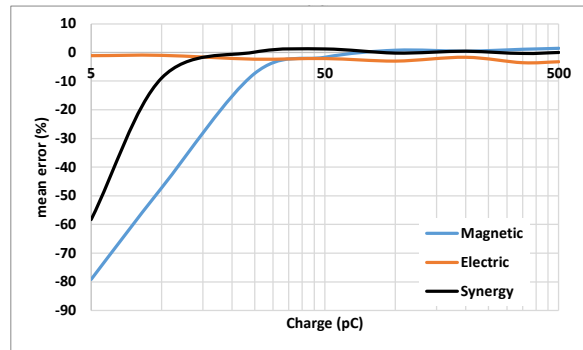
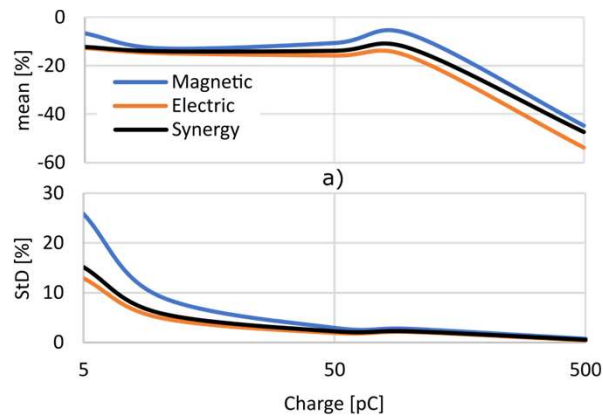
Calibration procedure.



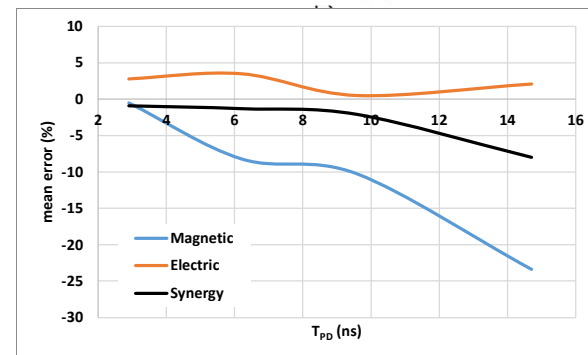
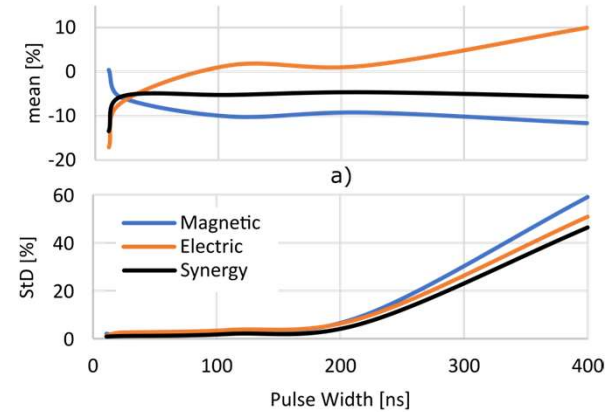
Calibration constant measurement for electric (top) and magnetic (bottom) antenna.

## 5.1 LV validation

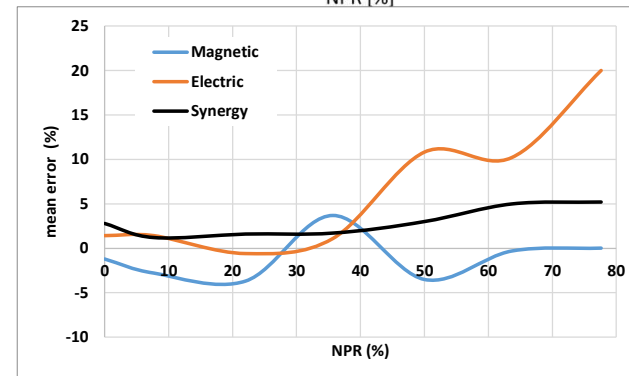
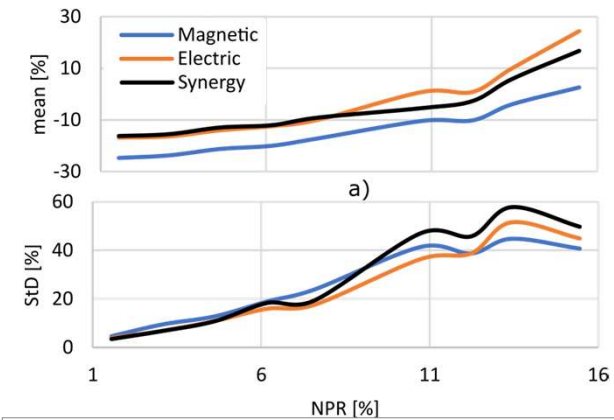
- Charge estimation uncertainty in the LV test bench.
  - Magnitude linearity
  - Pulse time with
  - Noise to signal ratio



a) Mean and b) standard deviation error with different charge inputs.



a) Mean and b) standard deviation error with different pulse lengths inputs.



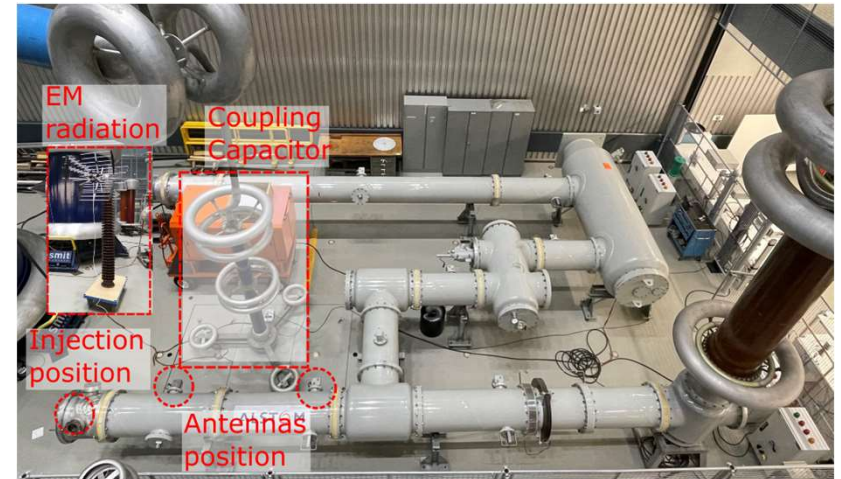
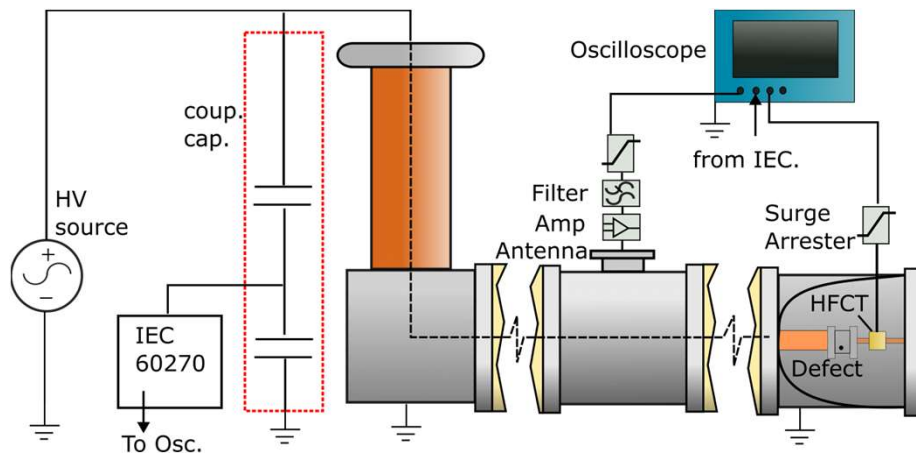
a) Mean and b) standard deviation error with different NPR inputs.

## 6.2.1 HV Validation

- HV test bench for characterization and validation of magnetic antenna.

### Parameters

- Voltage sources:
  - AC
  - DC + and -
- Defects:
  - Corona
  - moving particle
  - surface discharge
  - floating electrode
- Noises:
  - Random noise
  - CM pulses
  - EM radiation



## 6.2.2 HV Validation

		IEC limit	IEC/HFCT		MA/HFCT		EA/HFCT		Syn/HFCT		
			$\mu$ [%]	$\sigma$ [%]	$\mu$ [%]	$\sigma$ [%]	$\mu$ [%]	$\sigma$ [%]	$\mu$ [%]	$\sigma$ [%]	
Jumping Particle	AC	A4	10%	13	2	-42	3	-19	3	-27	2
		A1	10%	12	6	-35	8	-45	3	-34	5
	DC+	A4	10%	2	3	-25	2	-14	3	-12	2
		A1	10%	4	3	-18	2	-25	2	-13	2
	DC-	A4	10%	3	3	-30	2	-12	2	-13	2
		A1	10%	0	3	-16	2	-24	2	-10	2
FE	AC	A4	10%	29	8	-25	4	-9	4	-8	4
		A1	10%	20	27	-22	5	-24	5	-20	5
	DC-	A4	10%	328	356	-46	23	-36	27	-35	28
		A1	10%	240	336	-32	20	-39	18	-29	20
Corona	AC	A4	66%	72	39	-14	55	-6	15	-19	31
		A1	37%	86	49	-27	24	-38	13	-27	18
	DC+	A4	66%	144	64	-16	52	-17	16	-21	29
		A1	63%	164	83	9	86	-42	17	-32	37
	DC-	A4	49%	81	61	9	94	-17	21	-29	28
		A1	38%	71	36	-24	31	-34	12	-28	19
SD	AC	A4	20%	-2	33	-34	22	-29	13	-31	14
		A1	16%	-11	27	-43	15	-38	11	-37	13

TU Delft Results

Defect	HV Source	Magnetic Antenna		Electric Antenna		Synergy Method	
		$\mu$ (%)	$\sigma$ (%)	$\mu$ (%)	$\sigma$ (%)	$\mu$ (%)	$\sigma$ (%)
SD	AC	-32	9	-10	10	6	12
	AC	-15	5	20	6	-1	5
FE	DC+	18	5	23	4	-5	4
	DC-	15	8	15	5	-8	5
JP	AC	-28	22	-12	38	-7	31
	DC+	-15	21	2	25	-25	33
	DC-	-18	26	5	27	-28	33
Protusion	AC	-19	17	-76	8	-19	16

LCOE Results

Defect	HV Source	Reference	Noise	Magnetic Antenna		Electric Antenna	
				$\mu$ (%)	$\sigma$ (%)	$\mu$ (%)	$\sigma$ (%)
Protusion	DC-	HFCT	No Noise	-20	23	-8	19
FJP	DC-	IEC	No Noise	6	69	-7	31
FJP	DC-	IEC	N1	17	23	-10	28
FJP	DC-	IEC	N2	18	23	-1	27

SGI Results

## Conclusions

- Alternative method for measuring calibrated PD in GIS.
- Its contactless functionality allows its use for online monitoring.
- Allows wave shape construction for defect clustering.
- Calibration method for on-site substations.
- PD charge estimation sensitive to non-impulsive noise, increasing the measurement uncertainty.

### Future work

- Noise rejection method to improve the SNR.
- Interference rejection method.

## Thanks for your attention

Funded by: the EMPIR program by the Participating States and from the European Union's Horizon 2020 research and innovation program.

**Questions?**

